Genistein inhibits African swine fever virus replication *in vitro* by disrupting viral DNA synthesis

Erik Arabyan[a], Astghik Hakobyan[a], Armen Kotsinyan[a], Zaven Karalyan[b], Vahram Arakelov[c,d], Grigor Arakelov[c,d], Karen Nazaryan[c,d], Anna Simonyan[e], Rouben Aroutiounian[e], Fernando Ferreira[f,1], Hovakim Zakaryan[a,*,1]

[a] *Group of Antiviral Defense Mechanisms, Institute of Molecular Biology of NAS, 0014, Yerevan, Armenia*
[b] *Laboratory of Cell Biology and Virology, Institute of Molecular Biology of NAS, 0014, Yerevan, Armenia*
[c] *Laboratory of Computational Modeling of Biological Processes, Institute of Molecular Biology of NAS, 0014, Yerevan, Armenia*
[d] *Russian-Armenian (Slavonic) University, 0051, Yerevan, Armenia*
[e] *Department of Genetics and Cytology, Yerevan State University, 0025, Yerevan, Armenia*
[f] *Center for Interdisciplinary Research in Animal Health, Faculty of Veterinary Medicine, University of Lisbon, 1300-477 Lisbon, Portugal*

ARTICLE INFO

ABSTRACT

African swine fever virus (ASFV) is the causal agent of a highly-contagious and fatal disease of domestic pigs, leading to serious socio-economic consequences in affected countries. Once, neither an anti-viral drug nor an effective vaccines are available, studies on new anti-ASFV molecules are urgently need. Recently, it has been shown that ASFV type II topoisomerase (ASFV-topo II) is inhibited by several fluoroquinolones (bacterial DNA topoisomerase inhibitors), raising the idea that this viral enzyme can be a potential target for drug development against ASFV. Here, we report that genistein hampers ASFV infection at non-cytotoxic concentrations in Vero cells and porcine macrophages. Interestingly, the antiviral activity of this isoflavone, previously described as a topo II poison in eukaryotes, is maximal when it is added to cells at middle-phase of infection (8 hpi), disrupting viral DNA replication, blocking the transcription of late viral genes as well as the synthesis of late viral proteins, reducing viral progeny. Further, the single cell electrophoresis analysis revealed the presence of fragmented ASFV genomes in cells exposed to genistein, suggesting that this molecule also acts as an ASFV-topo II poison and not as a reversible inhibitor. No antiviral effects were detected when genistein was added before or at entry phase of ASFV infection. Molecular docking studies demonstrated that genistein may interact with four residues of the ATP-binding site of ASFV-topo II (Asn-144, Val-146, Gly-147 and Leu-148), showing more binding affinity (-4.62 kcal/mol) than ATP^{4-} (-3.02 kcal/mol), emphasizing the idea that this viral enzyme has an essential role during viral genome replication and can be a good target for drug development against ASFV.

1. Introduction

African swine fever virus (ASFV), the only member of the family *Asfarviridae*, is an enveloped virus that contains a 170–193 kbp double-stranded DNA encoding more than 150 genes. It is the causative agent of African swine fever (ASF), a highly contagious transboundary disease of domestic and wild pigs. Depending on circulating viral strain, clinical signs may vary from the highly lethal form with 100% mortality to subclinical and asymptomatic forms (Gallardo et al., 2015). Although ASF was eradicated from Europe (except Sardinia) in 1995, it was re-emerged in the Caucasus region in 2007 and has spread to the Russian Federation, Ukraine, Belarus, Estonia, Latvia, Lithuania, Poland and Moldova, causing serious socio-economic impact on affected countries (Gallardo et al., 2015). The fact that no vaccine is available makes antiviral research a strong priority in the ASFV field (Zakaryan and Revilla, 2016).

Flavonoids or polyphenolics are secondary metabolites found in vegetables, fruits, seeds, nuts, spices, stems as well as in red wine and tea. They have a broad spectrum of biological activities such as neuroprotective, antioxidant, anti-inflammatory, anticancer, and antibacterial (Romano et al., 2013). Interestingly, one of the many biological effects of flavonoids is their antiviral activity. For example, apigenin extracted from *Ocimum basilicum* showed a potent antiviral activity against adenoviruses and hepatitis B virus (Chiang et al., 2005),

whereas quercetin demonstrated a dose-dependent antiviral activity against herpes simplex virus (Lyu et al., 2005), Japanese encephalitis virus (Johari et al., 2012), hepatitis C virus *in vitro* (Rojas et al., 2016); and influenza A subtypes *in vivo* (Cho et al., 2015). Similarly, genistein was shown to inhibit HIV infection in resting CD4 T cells through interference with HIV-mediated actin dynamics (Guo et al., 2013). It also disrupted replication of avian leucosis virus, rotavirus and herpes simplex virus *in vitro* (Argenta et al., 2015; Huang et al., 2015; Qian et al., 2014).

We have recently found that two flavonoids, apigenin and genistein, exerted inhibitory effect on the replication of ASFV *in vitro* (Hakobyan et al., 2016). However, the anti-ASFV mechanisms of genistein were not investigated. Here we reported a dose-dependent inhibition of ASFV in Vero cells and porcine alveolar macrophages. We also demonstrated that the major antiviral effect was observed when genistein was added at time point coincided with the viral DNA synthesis, suggesting that this event could be impaired by genistein. Further experiments confirmed that genistein inhibited viral DNA replication and protein synthesis. Finally, based on the results obtained from comet assay and molecular docking, we proposed a mechanism of action for the antiviral activity of genistein.

2. Materials and methods

2.1. Cells, virus and drugs

Vero (African green monkey kidney) cells were maintained at 37 °C in Eagle's minimum essential medium (EMEM) (Lonza, Belgium) supplemented with 10% of fetal bovine serum (FBS), 2 mM L-glutamine, 100 IU/ml penicillin and 100 μg/ml streptomycin (all from Sigma-Aldrich, Germany). Preparation of porcine alveolar macrophages was done as previously described (Carrascosa et al., 2011). Alveolar cells were cultured at 37 °C in Dulbecco's Modified Eagle's Medium (DMEM) (Sigma-Aldrich, Germany) supplemented with 10% of FBS, 2 mM L-glutamine, 100 IU/ml penicillin and 100 μg/ml streptomycin. In experiments with Vero cells, the Vero-adapted ASFV Ba71V strain was used. For ASFV Ba71V strain, the viral titration was measured by cytopathic effect (CPE-based) assay on Vero cells by 10-fold serial dilutions of supernatants. The titer was calculated by Spearman-Kärber endpoint method and expressed as $TCID_{50}/ml$. Porcine alveolar macrophages were infected by the virulent ASFV Armenia/07 strain. The titration of this strain was performed by hemadsorption (HAD) assay as previously described (Carrascosa et al., 2011). The titer was expressed as $HADU_{50}/ml$.

Genistein was purchased from Cayman Chemical (Germany). It was dissolved in dimethyl sulfoxide (DMSO) as 20 mM stock and resuspended in EMEM without FBS at indicated concentrations for further use. At the time of experiments, dilutions in cell culture medium were performed with the final concentration of DMSO not exceeding 1% (v/v).

2.2. Cytotoxicity

The cytotoxicity of genistein was evaluated in Vero cells and porcine alveolar macrophages by MTT assay. Confluent cells in 96-well cell culture plate (2×10^4 cell/well) were treated with increasing concentrations of the genistein ranging from 12.5 to 200 μM. Treated cells were incubated for 96 h at 37 °C in 5% CO_2. After incubation, medium was removed and MTT solution (Sigma-Aldrich, Germany) was added. Cells were incubated at 37 °C for 4 h after adding MTT solution, followed by purple formazan extraction by MTT solvent. The colorimetric measurements were performed on a microplate reader at 570 nm. (Tecan Spectra II, Switzerland) The percentage of viable cells was calculated for each concentration as $[(OD_T/OD_C) \times 100]$, where OD_T and OD_C were correspond to the absorbance of treated and control cells, respectively. The 50% cell cytotoxicity (CC_{50}) was determined as the

concentration of compounds, which causes 50% cellular death. The cytotoxicity of the final concentration of DMSO was also measured.

2.3. Yield reduction assay

Vero cells in 24-well cell culture plate (2×10^5 cell/well) and macrophages (4×10^4 cell/well) in 96-well plate were incubated with ASFV Ba71V (0.5 $TCID_{50}/cell$) or ASFV Armenia/07 strain (0.5 $HADU_{50}/cell$). Genistein was added at decreasing concentrations (from 50 μM to 3.12 μM). After 1 h, the virus inoculum was removed and new medium with tested compound was added. Virus was collected at 96 hpi and titrated by CPE-based assay or by HAD assay.

2.4. Time-of-addition assay

Vero cells in 24-well cell culture plate (2×10^5 cell/well) and macrophages (4×10^4 cell/well) in 96-well plate were designed as −2, 0, 2, 8 and 16 h, according to the time of ASFV infection. In pre-treatment assay, Vero cells and macrophages were treated with genistein for 2 h before infection with ASFV Ba71V (0.5 $TCID_{50}/cell$) and ASFV Armenia/07 (0.5 $HADU_{50}/cell$), respectively. In co-treatment assay, cells were exposed with genistein at the same time that ASFV was added to the cells. In post-treatment assay, cells were infected with ASFV, and the compound was added at 2, 8 and 16 h after infection. For the virus control, ASFV was added to the respective wells at 0 h. The plate was then incubated at 37 °C in 5% CO_2 for 96 h. The virus was collected and titrated by CPE-based assay or by HAD assay.

2.5. Anti-entry assays

For the attachment assay, Vero cells in 24-well cell culture plate (2×10^5 cell/well) were incubated with ASFV (0.5 $TCID_{50}/cell$) and genistein at 4 °C for 1 h to allow virus binding but prevent viral internalization. Unbound virus and genistein were then discarded, cells were thoroughly washed by PBS and EMEM containing 3% FBS was added. The plate was then switched to 37 °C and incubated for 24, 48 and 96 h.

For internalization assay, cells were incubated with ASFV at 4 °C for 1 h. Then, unbound virus was discarded, cells were thoroughly washed by PBS and the temperature was shifted to 37 °C to allow virus entry proceed. The tested compound was added at 0 h and removed at 1 h following temperature shift. Then, cells were thoroughly washed by PBS before fresh EMEM was added. The time point, when cells were shifted to 37 °C was considered as 0 h. After 24, 48 and 96 h, the virus was collected and titrated by CPE-based assay.

2.6. Virucidal assay

The virus suspension containing 2×10^5 $TCID_{50}/well$ particles was incubated with volume solution of genistein (50 μM), for 1 h at 37 °C. Then, Vero cells in 96-well cell culture plate (2×10^4 cell/well) were infected with the 20-fold diluted treated viral suspension to eliminate the potential effects of genistein on ASFV infection. After 1 h adsorption at 37 °C, cells were thoroughly washed with PBS and EMEM containing 3% FBS was added. After 24, 48 and 96 h, the virus titer was analyzed by CPE-based assay.

2.7. Quantification of viral DNA in ASFV factories

Viral DNA measurements were done as previously described (Hakobyan et al., 2016). Briefly, Vero cells and macrophages grown on coverslips (3×10^5 cell/well) and infected with ASFV BA71V (2 $TCID_{50}/cell$) and ASFV Armenia/07 (2 $HADU_{50}/cell$), respectively, were exposed to genistein (50 μM) from 0 hpi or from 8 hpi. At 16 hpi, cells were fixed in a 96% ethanol solution for 30 min and stained in fresh Schiff's reagent (DNA hydrolysis in 5 N hydrochloric acid, 60 min at 22 °C) by the method of Feulgen. The DNA content of viral

factories was measured by computer-equipped microscope-cytometer SMP 05 (Carl Zeiss, Germany) at 575 nm and expressed as Integrated Optical Density (IOD), the cytometric equivalent of DNA content. The measurement was carried out for 100 viral factories per sample.

2.8. Western blotting analysis

Vero cells and porcine macrophages grown in 30 mm dishes were infected with ASFV-Ba71V strain (MOI of 1) or with ASFV Armenia/07 (MOI of 0.5) and when indicated, exposed to genistein (Sigma-Aldrich) at 5, 10, 50 μM concentrations, after the adsorption period (1 h). Following this step and before protein extraction, mock-infected, infected and genistein-treated infected-cells were washed twice with PBS and then lysed in ice-cold modified RIPA buffer (25 mM Tris, 150 mM NaCl, 0.5% (v/v) NP40, 0.5% (w/v) sodium deoxycolate, 0.1% (w/v) SDS, pH 8.2) supplemented with protease-inhibitor cocktail (cOmplete, Mini, EDTA-free, Roche) and phosphatase-inhibitor cocktail (PhosStop, Roche). Clarified whole-cell lysates harvested at 16 hpi, were subjected to SDS-PAGE gel electrophoresis using 8–16% (w/v) polyacrylamide separating gels (Bio-Rad), and transferred to a 0.2 μm pore diameter nitrocellulose membrane (Whatman Schleider & Schuell) by electro-blotting. Blot membranes were then blocked with phosphate-buffered saline plus 0.05% (v/v) Tween-20 (PBST), containing 5% (w/v) of BSA (Sigma-Aldrich), during 1 h at RT, and thereafter incubated with specific primary antibodies (RT, 1 h), followed by a wash step with PBST (3×10 min). Then, membranes were incubated with appropriate secondary antibodies conjugated with HRP, for 1 h at RT. A final wash step in PBST (3×10 min) was performed before protein detection with a chemiluminescence detection kit (Pierce® ECL Western Blotting Substrate, Thermo Scientific), on Amersham Hyperfilm ECL (GE Healthcare), and α-tubulin was used as a loading control. For immunoblotting analysis, the following primary antibodies were used: an in-house produced swine anti-ASFV serum (1:200), an anti-VP73 (1BC11) from Ingenasa, Madrid, Spain and an anti-α-tubulin (# 2125, 1:200) from Cell Signalling Technology. All dilutions were performed in blocking solution diluted and incubated according to manufacturers' recommendations. The following HRP-conjugated antibodies were incubated during a 30 min period at user's improved concentrations: anti-swine IgG (114-035-003, 1:100.000), anti-rabbit IgG (111-035-003, 1:50.000) and anti-mouse IgG (315-035-003, 1:75.000) all from Jackson ImmunoResearch Lab., West Grove, USA.

2.9. Quantitative reverse transcription PCR (qRT-PCR)

qRT-PCR analysis was performed as previously described (Frouco et al., 2017). Briefly, total RNA was extracted from ASFV-infected porcine macrophages (MOI of 0.5) at different time points of infection, using the RNeasy Mini Kit and RNase-free DNase Set, both from Qiagen. First-strand cDNA was synthesized from 3 μg of total RNA, using the Superscript II First Strand Synthesis System (Invitrogen) and analyzed in duplicate by qRT-PCR. The real-time PCR reaction mixtures contained 1 μl (1:10) of template cDNA, 2.5 μl of forward and reverse primers (at 50 nM, Table 1), 12.5 μl of Maxima SYBR Green/ROX qPCR

Master Mix (Thermo Scientific) and sterile water to a final volume of 25 μL per tube. The thermal cycling conditions were an initial denaturation step of 95 °C for 10 min, followed by 40 cycles of 95 °C for 10 s and 60 °C for 60 s qRT-PCR analysis was performed using the 7300 Real-Time PCR System (from Applied Biosystems) and the mRNA levels of viral genes (A104R, CP204L and B646L) and of the reference gene (Cyclophilin A) were quantified using the standard curves of different plasmids (pGEM®-Teasy_A104R, pGEM®-Teasy_CP204L, pGEM®-Teasy_B646L and pGEM®-Teasy_Cyclophilin A). Only data from qRT-PCR reactions showing an amplification efficiency ≥ 0.95 and $R2 \geq 0.98$ were used.

2.10. Comet assay

The level of DNA damage was evaluated by standard alkaline comet assay (Tice et al., 2000; Freitas et al., 2016). Vero cells (4×10^5 cell) infected with ASFV Ba71V (5 $TCID_{50}$/cell) were exposed to genistein (50 μM) from 1 to 14 hpi, 8 to 14 hpi and 13 to 14 hpi. In addition, non-infected and non-exposed, non-infected but exposed, and infected but non-exposed cell cultures were used as controls. A mixture of 20 μL of cells with 80 μL of low melting point agarose (0.5%) was placed on a slide precoated with 1% normal melting point agarose. The cells were then lysed by immersing the slides in lysis solution (2.5 M NaCl, 100 mM Na_2EDTA, 10 mM Tris and 1% Triton X-100, pH 10.0) for 60 min at 4 °C, incubated in freshly made alkaline buffer (300 mM NaOH and 1 mM Na_2EDTA, pH 13.0) for 20 min in electrophoresis tank for DNA unwinding, and electrophoresed for 15 min at 300 mA (1 V/cm) in the same buffer. Slides were neutralized with 0.4 M Tris, pH 7.5 for 15 min and stained with 20 μg/mL ethidium bromide. The images were examined by fluorescence microscope (ZEISS, Germany). DNA damage was assessed using a Comet Assay IV software (Perceptive Instruments, UK). A total of 150 cells were analyzed in three replicated slides for each sample. % DNA tail was used to quantify the DNA damage.

2.11. In silico experiments

Homology modeling of ASFV-topo II tertiary structure was conducted using ICM-PRO 3.8–7 program package with full refinement option in the ICM force field (Abagyan et al., 1994). The amino acid sequence of ASFV-topo II was retrieved from UniProtKB (ID: Q00942) and was used for homology modeling. Close homologues with available crystal structures in the Protein Databank were identified using ICM. The crystal structure of topo II dimer from *Saccharomyces cerevisiae* (PDB: 4GFH) and the crystal structure of human topo II-α (PDB: 4FM9) had the highest similarity (4GFH – 27%, 4FM9 – 30%) and coverage (4GFH – 98%, 4FM9 – 47%) relatively to ASFV-topo II from all available homologues crystal structures. They were identified as the most suitable template candidates for homology modeling. For determining the accuracy of the obtained model PROCHECK program was used (Laskowski et al., 1993). Since ASFV-topo II binds two Mg^{2+} ions per subunit, which are its cofactors, we conducted induced fit docking of two Mg^{2+} ions on the ASFV-topo II monomer model.

Table 1
Sequence of the primers used in qRT-PCR analysis.

| Target	Primer name	Sequence Sense Sequence (5′- 3′)	Orientation
ASFV-A104R	A104R_Fw	ACCCGGAATCAAGTTCACCG	Forward
ASFV-A104R	A104R_Rev	CGGCTTTATGTTCAGGCTTGG	Reverse
ASFV-B646L	VP72_Fw	ACGGCGCCCTCTAAAGGT	Forward
ASFV-B646L	VP72_Rev	CATGGTCAGCTTCAAACGTTTC	Reverse
ASFV-CP204L	VP32_Fw	TGCACATCCTCCTTTGAAACAT	Forward
ASFV-CP204L	VP32_Rev	TCTTTTGTGCAAGCATATACAGCTT	Reverse
Cyclophilin A	Cyclo_Fw	AGACAAGGTTCCAAAGACAGCAG	Forward
Cyclophilin A	Cyclo_Rev	AGACTGAGTGGTTGGATGGCA	Reverse
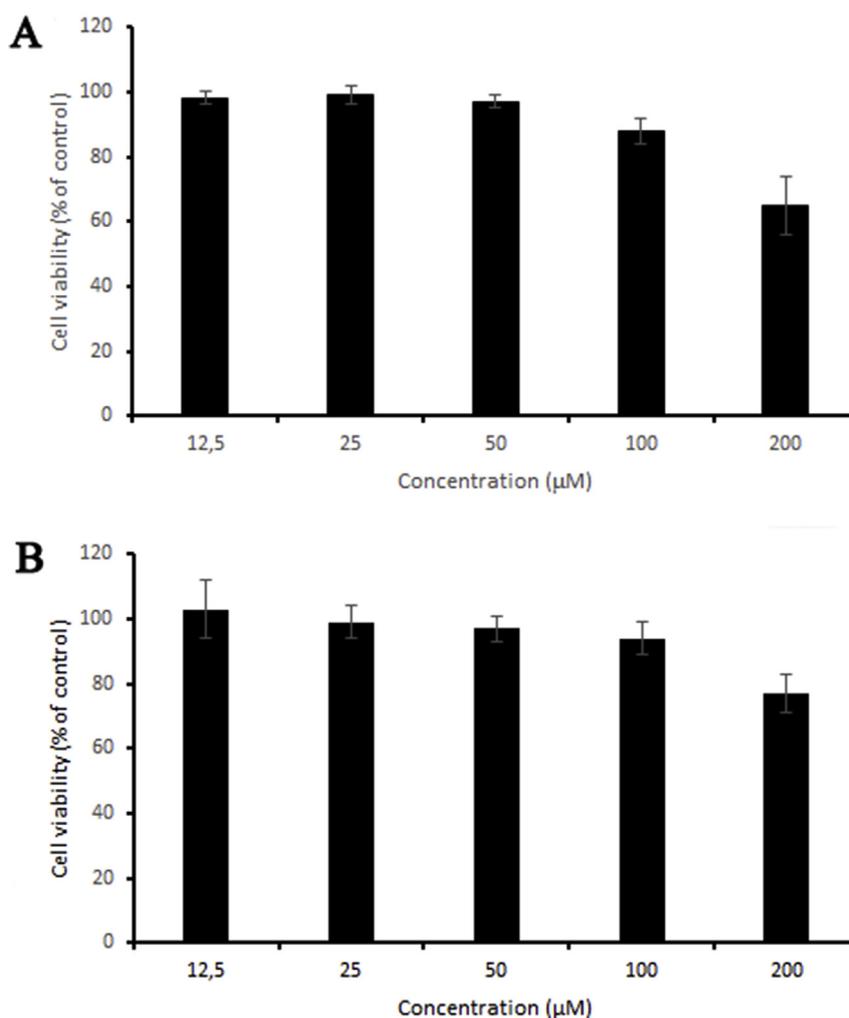
Fig. 1. Cytotoxicity of genistein on Vero (A) cells and porcine macrophages (B). Dose-dependent cytotoxicity was evaluated by MTT assay. Values represent mean and standard deviation results from three independent experiments.

Protein-protein docking of obtained ASFV-topo II monomer tertiary structure with itself was carried out and repeated 10 times using Fast Fourier Transform (FFT) docking method of ICM (Totrov and Abagyan, 1997), followed by refinement procedure of the best obtained dimer model. Final refined ASFV-topo II dimer model was solvated in water, followed by neutralization of the system and subjected to SD and ABNR minimization algorithm in the CHARMM c36m force field using the CHARMM 42b1 program (Brooks et al., 1983).

The structures of ATP^{4-} and genistein were obtained from the MolCart compounds database of ICM. Induced fit docking of ATP^{4-} and genistein with ASFV-topo II dimer model using ICM Explicit Group Docking method was performed (Fernandez-Recio et al., 2005). The docking of each compound was repeated 300 times. The docking results were evaluated by ICM score values. For the best interaction models, binding energies were also evaluated (Schapira et al., 1999). Visualization and analysis of the ASFV-topo II dimer model and docking results were performed using the ICM-PRO. All software packages were used in the Linux OSon the computer cluster of the IMB NAS RA and on HPC of MSU.

2.12. Statistics

The CC_{50} was calculated by a linear regression analysis of dose-response curves generated from the data. The IC_{50} was calculated by a nonlinear regression analysis of dose-response curves generated from the data. Data are expressed as mean ± SD of three independent experiments. Data were analyzed by non-parametric Mann-Whitney *U* test for comet assay and by Student's *t*-test for other assays. $P < 0.05$ was considered to be statistically significant.

3. Results

3.1. Evaluation of the cytotoxicity of genistein

The cytotoxicity of genistein was measured based on MTT assay and carried out when Vero cells and porcine alveolar macrophages were exposed to genistein for 4 days. This time interval was chosen because virus yield reductions were also measured after a 4-day incubation period, when complete CPE was observed. As shown in Fig. 1A, genistein inhibited Vero cells growth at concentrations above 50 μM and the cytotoxic concentration 50 (50% of cell survival or CC_{50}) was 298.7 μM. The cytotoxic effect of genistein on macrophages was lower than on Vero cells with $CC_{50} = 410.5$ μM (Fig. 1B). Cells treated with DMSO at concentration less than 1% (v/v) did not display cytotoxic changes (data not shown).

3.2. Antiviral effect of genistein on ASFV infection in Vero cells

To establish whether genistein possesses antiviral activity against ASFV in a dose-dependent manner, we treated ASFV-infected Vero cells with genistein at different concentrations ranging from 3.12 μM to 50 μM. As shown in Fig. 2A, genistein exerted anti-ASFV effect in a
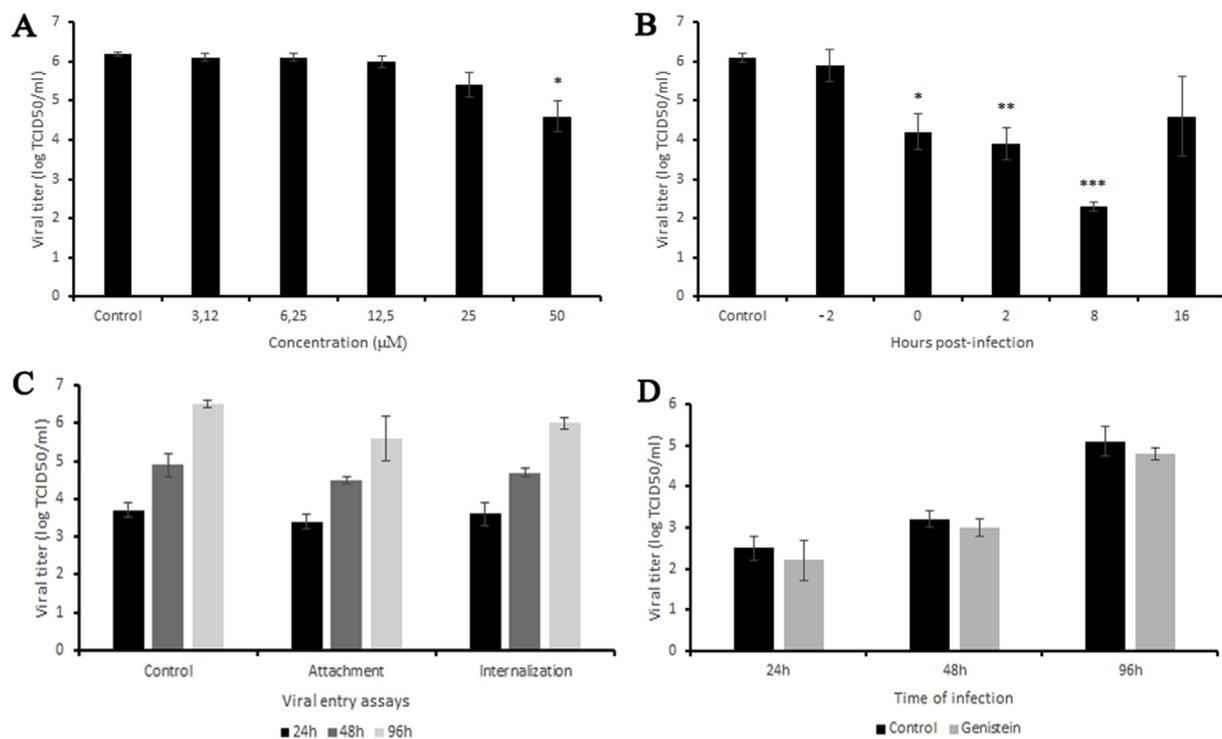
Fig. 2. Evaluation of the anti-ASFV activity of genistein. (A) ASFV yield in Vero cells treated with genistein in several concentrations. Genistein was added at 0 hpi. (B) Antiviral effect of genistein depending on the time of addition. (C) Effect of genistein treatment on ASFV entry. (D) Virucidal effect of genistein on extracellular ASFV particles. Concentration of genistein in B, C, and D assays was 50 μM. Infected cells incubated with DMSO containing medium were used as control. Values represent mean and standard deviation results from three independent experiments. Significant differences compared to control are denoted by *($P < 0.05$), **($P < 0.02$) and ***($P < 0.001$).

dose-dependent manner (IC$_{50}$ = 13 μM, SI = 23). It reduced the viral yield from 6.2 $\pm$ 0.05 log TCID$_{50}$/ml to 4.6 $\pm$ 0.4 TCID$_{50}$/ml at 50 μM concentration ($P < 0.05$), not exhibiting a significant antiviral effect at concentrations lower than 25 μM. Since the compound showed potent inhibitory activity at 50 μM concentration, we decided to perform further evaluation using this concentration.

Next, we conducted time-of-addition assay to evaluate the effect of genistein on specific step(s) of the ASFV life cycle. Therefore, the compound was added at 2 h prior infection (pre-treatment) and 0, 2, 8 and 16 h post-infection (hpi) (post-treatment). The data shown in Fig. 2B suggest that genistein exhibited the most potent anti-ASFV activity, when it was added at 8 hpi. It reduced the viral titer by 3.8 log (> 99%, $P < 0.001$). The strong antiviral effect was also observed, when genistein was added at 0 and 2 hpi ($P < 0.05$). In contrast, genistein showed no inhibitory effect on ASFV infection, when cells were treated before infection. Taken together, these results indicate that early and middle stages of ASFV infection can be disrupted by genistein.

Based on the results of time-of-addition assay, we speculated that genistein could act either as a virucidal agent or through blocking viral entry. Therefore, we studied the effect of genistein on viral entry, as well as on extracellular viral particles (virucidal activity). As shown in Fig. 2C and D, neither anti-entry nor virucidal effects of genistein were detected, when virus yield was quantified at different hours post-infection.

3.3. Effect of genistein on viral DNA and protein synthesis in Vero cells

Since the major anti-ASFV effect occurred when genistein was added at 8 hpi, which coincided in time with the early stages of viral DNA synthesis (Rojo et al., 1999; Simões et al., 2015), we hypothesized that genistein may inhibit ASFV infection by targeting the viral DNA replication. In order to prove this idea, we performed image cytometry

to quantify ASFV DNA in viral factories (Fig. 3A). A significant reduction (34%, $P < 0.05$) in the amount of viral DNA was found, when ASFV-infected cells were exposed to genistein from 0 hpi (Fig. 3B). Moreover, the decrease in viral DNA was higher (54%, $P < 0.02$), when ASFV-infected cells were treated with genistein at 8 hpi. These results suggest that the viral DNA synthesis is impaired in the presence of genistein.

Knowing that genistein reduces the viral yield, we also investigated whether ASFV protein synthesis was blocked by detecting the expression of an early (p32) and a late (p72) viral protein via western blot. The results showed that the synthesis of both proteins was significantly reduced following treatment with genistein, and this inhibition occurred in a dose-dependent manner (Fig. 3C). Together, our data indicate that genistein inhibits post-entry stages of ASFV life-cycle.

3.4. Interaction of genistein with ASFV-topoisomerase II enzyme

ASFV encodes a protein with type II topoisomerase (topo II) activity (Coelho et al., 2015). Previous studies showed that genistein inhibited the activity of ASFV-topo II, which was heterologously expressed in *Saccharomyces cerevisiae* (Coelho et al., 2016). Here we studied the effect of genistein on ASFV-topo II during viral infection using a single cell electrophoresis analysis (comet assay) (Fig. 4A). As shown in Fig. 4B, the presence of ASFV and genistein alone or in combination together contributed to DNA damage in comparison with non-infected and non-exposed control cells ($P < 0.001$ or $P < 0.02$). However, DNA fragmentation was three or four times higher, when ASFV-infected cells were exposed to genistein at intermediate-late phase of infection ($P < 0.001$), which is characterized by an increasing rate of viral DNA replication (Rojo et al., 1999).

To characterize the likely interaction between genistein and ASFV-topo II, we performed molecular docking analysis. In the absence of an available X-ray crystal structure of ASFV-topo II, we constructed ASFV-
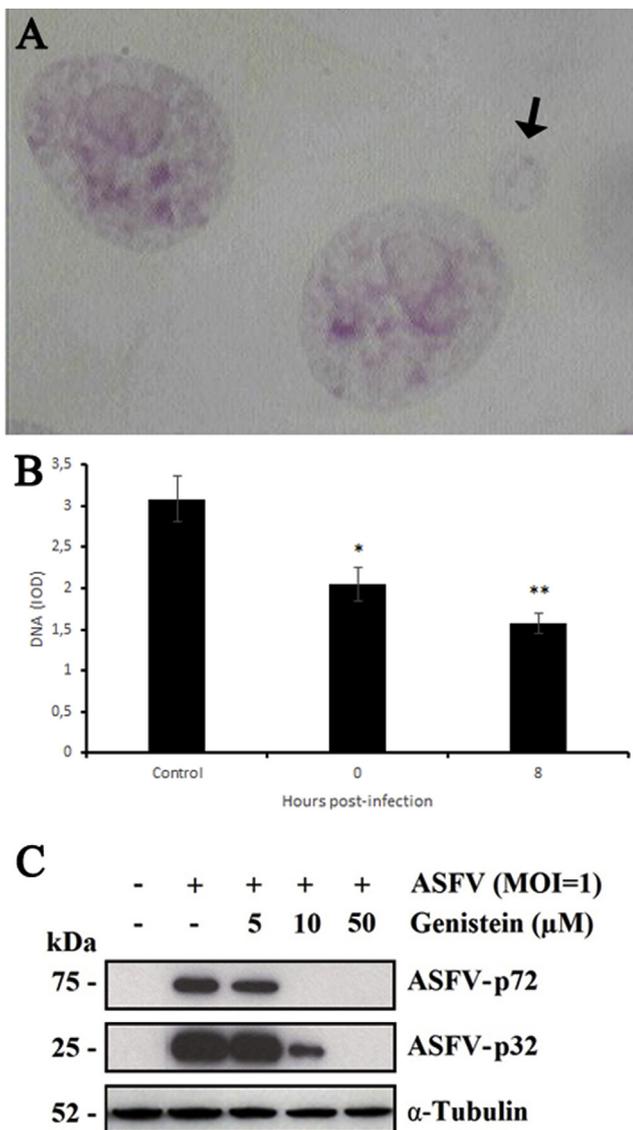
Fig. 3. Inhibition of viral DNA and protein synthesis. (A) Visualization of ASFV factory (indicated by arrow) in Vero cells by the method of Feulgen. (B) The DNA content of ASFV factories in genistein-treated cells. (C) Viral protein synthesis analyzed by Western blotting. α-tubulin was used as a loading control. Molecular weights (kDa) of evaluated proteins are indicated on the left of immunoblot image. For Western blotting, genistein was used at 5, 10 and 50 μM concentrations. Values represent mean and standard deviation results from three independent experiments. Significant differences compared to control are denoted by *($P < 0.05$) and **($P < 0.02$).

topo II homology model based on the structures of its close homologues. Homology modeling was followed by the process of reliability verification of the ASFV-topo II model tertiary structure. The stereochemical correctness of protein was carried out and the result of this test was visualized as a Ramachandran plot (Fig. 1S). Since topo II has two Mg^{2+} ions as cofactor per subunit, two Mg^{2+} ions were docked with the obtained ASFV-topo II model. After obtaining the ASFV-topo II tertiary structure model in complex with two Mg^{2+} ions, a protein-protein docking of the obtained model with itself was carried out. The crystal structure of DNA topoisomerase II dimer from *Saccharomyces cerevisiae* [PDB: 4GFH] was used as an object for evaluation. As a result of the protein-protein docking, 10^5 models were obtained of the ASFV-topo II dimer structure. The model with the lowest interaction energy (-106.1 kcal/mol) and the lowest RMSD (8.974 Å) compared with the 4GFH structure was chosen as the best one. The structure of the best

obtained ASFV-topo II dimer model in the complex with four Mg^{2+} ions was solvated by a water shell 7 Å thick around it. After that, the system was neutralized by Cl^-, Na^+ and Mg^{2+} ions in the concentration of 150 mM. The size of the resulting system was 101611 atoms (19158 -ASFV-TOPOII-A, 19158 -ASFV-TOPOII-B, 63138 - H_2O, 57 - Na^+, 95 - Cl^-, 5 - Mg^{2+}). The resulting system was subjected to 30,000 steps of a SD minimization algorithm and to 60,000 steps of ABNR minimization algorithm. The energy of the obtained system was -193785 kcal/mol. The final ASFV-topo II dimer model is presented in Fig. 4C. For docking analysis, we selected all amino acids in the ATP-binding site (16 amino acids) as possible interaction sites with genistein. The top ranking model based on the smallest ICM score value and visual analysis is shown as 3D snapshot and 2D plot of genistein interacting side chains of the ASFV-topo II dimer model (Fig. 4D). Genistein formed hydrogen bonds with the ATP-binding site residues Asn-144, Val-146, Gly-147 and Leu-148. Binding energy values revealed that genistein bound to the ATP-binding site (-4.62 kcal/mol) with more affinity as compared to ATP^{4-} (-3.02 kcal/mol) (Table 2) (Fig. 2S), suggesting that genistein could effectively compete with ATP^{4-} for the binding site.

3.5. Inhibition of ASFV infection in porcine macrophages

Since the ATP-binding site residues are conserved among different ASFV strains (Fig. 3S), we expected that genistein should have the same antiviral effect on other ASFV strains. Therefore, we conducted additional experiments to test the inhibitory activity of genistein against the virulent ASFV strain in porcine macrophages, the natural host cells. As shown in Fig. 5A, genistein inhibited ASFV infection in a dose-dependent manner, and it was not effective at concentrations lower than 50 μM ($P < 0.05$). The IC_{50} of genistein for ASFV Armenia/07 strain was higher ($IC_{50} = 17$ μM; SI = 24.1) than that reported for ASFV Ba71V. In agreement with previous observation, the strongest reduction (2.5 log; > 99%) in viral titer was found when genistein treatment was initiated at 8 hpi ($P < 0.001$) (Fig. 5B). The antiviral effect was less pronounced when genistein was added early or late in the replication cycle. No virucidal and anti-entry activity were observed (data not shown). Finally, a significant decrease (41%, $P < 0.02$) in the amount of viral DNA in ASFV factories was observed, when ASFV-infected macrophages were exposed to genistein at 8 hpi (Fig. 5C). Thus, the antiviral activity of genistein against ASFV Armenia/07 strain is similar to its effect on ASFV Ba71V strain.

3.6. Genistein inhibits viral transcription and protein synthesis in porcine macrophages

In order to further explore the antiviral effects of genistein, the expression of three viral genes was investigated and compared between non-treated and treated ASFV-infected porcine macrophages (Fig. 6A and B). A severe reduction in the viral transcription activity was detected in genistein-treated macrophages from 10 hpi onwards, with the viral transcripts being decreased up to 99.04%, at 20 hpi (ASFV-B646L, Fig. 6B). In parallel, immunoblot analysis showed that genistein also disrupts viral protein synthesis, in particular, the translation of late viral proteins (Fig. 6C), probably because at 8 hpi some p32 was already synthetized, corroborating the results obtained in Vero cells.

4. Discussion

Over the years, a large number of vaccines were tested against ASFV. However, none of them have been taken forward for commercial production (Zakaryan and Revilla, 2016; Arias et al., 2017). It is in this context that we conducted the antiviral screening of different compounds for the development of effective antiviral therapeutics (Hakobyan et al., 2016, 2018). One such compound, genistein, has been shown to inhibit replication of different viruses through diverse mechanisms. For instance, genistein inhibits human cytomegalovirus via
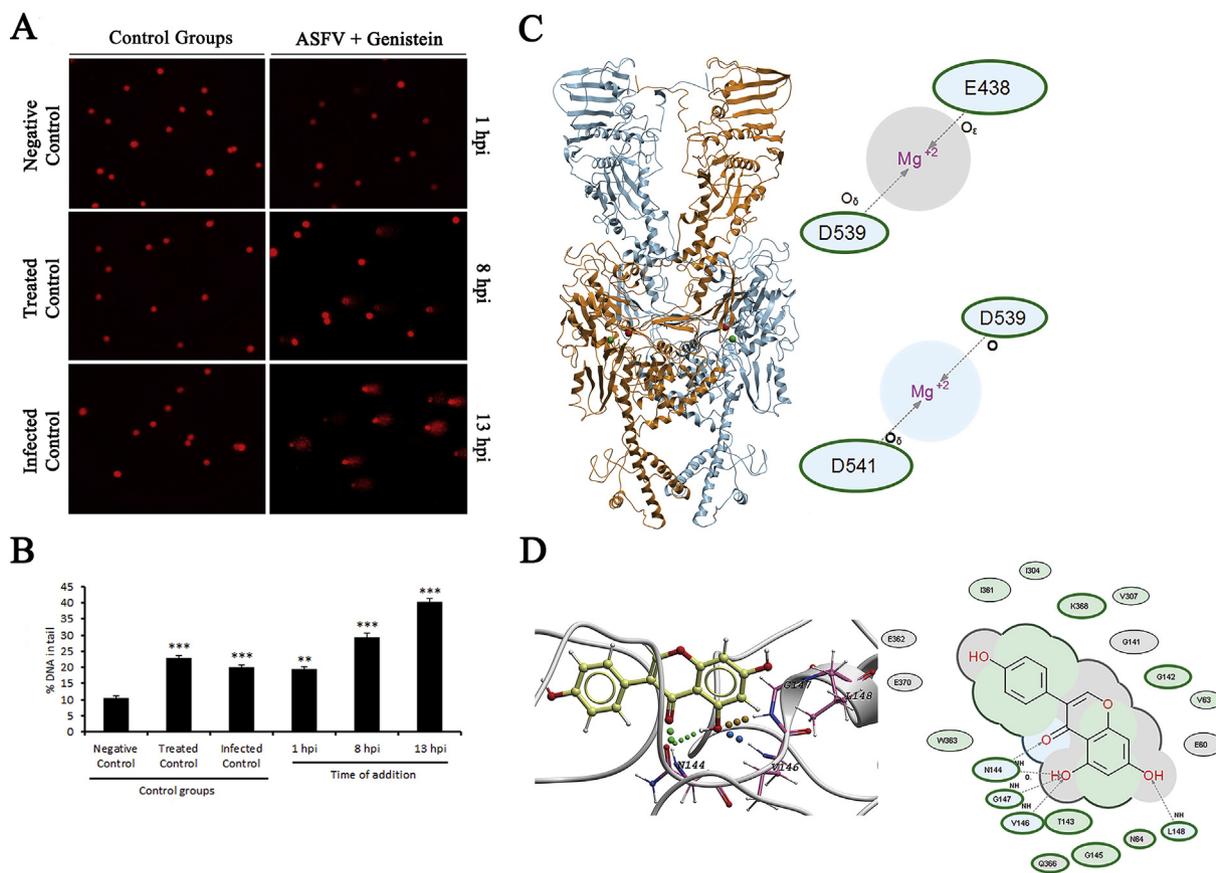
Fig. 4. Interaction of genistein with ASFV-topo II. (A) Genistein-induced DNA fragmentation analyzed by comet assay. (B) Analysis of % DNA in tail upon treatment with genistein. (C) Structure of ASFV-topo II dimer (left side) generated by homology modeling and 2D plot of Mg^{2+} interaction sites (right side). Two dimers are colored individually. Red and green circles are Mg^{2+} in dimer. (D) 3D snapshot of genistein interaction with ASFV-topo II dimer (left side) and 2D plot of genistein's interaction with ASFV-topo II dimer (right side). Hydrogen bonds are indicated by dash line. Significant differences compared to control are denoted by **($P < 0.02$) and ***($P < 0.001$). (For interpretation of the references to color in this figure legend, the reader is referred to the Web version of this article.)

Table 2
Binding energy, ICM score and interaction sites of ATP^{4-} and Genistein.

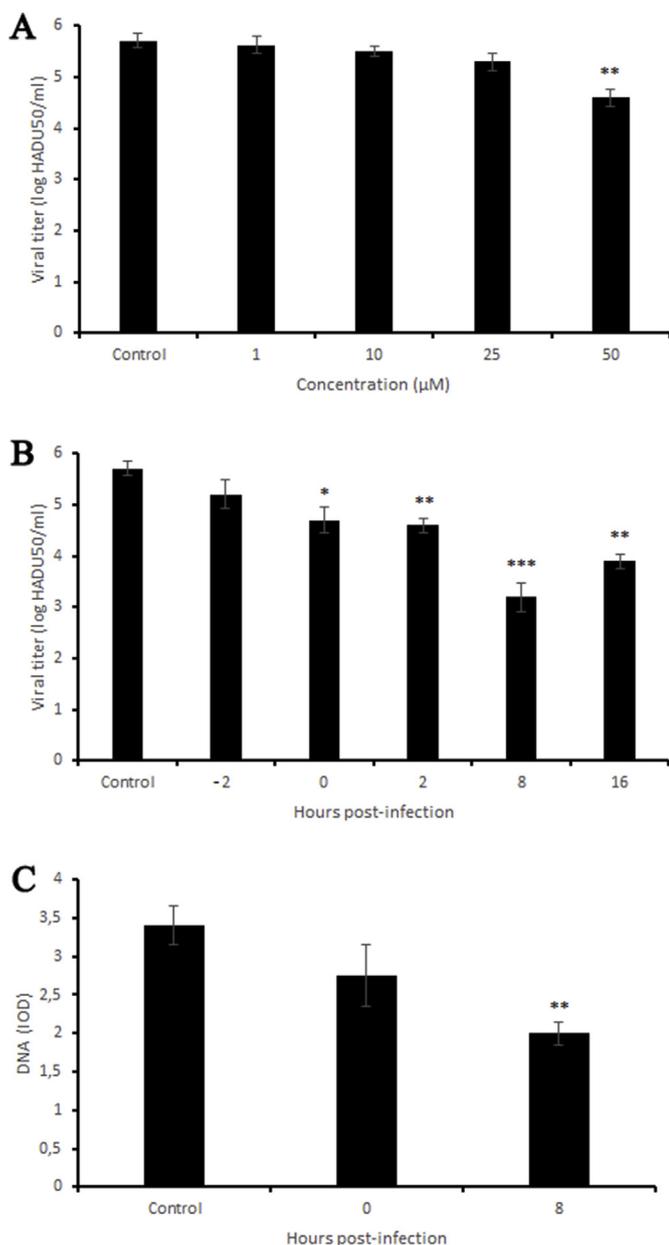| Docking against ASFV-topo II dimer model						
Compound	Binding energy (kcal/mol)	ICM score	H-bond		Hydrophobic interaction	
			Amino acid-ligand atom	Distance (Å)	Amino acid-ligand atom	Distance (Å)
ATP^{4-}	−3.02	−102.9	N64···O5	3.061	H68···C9	4.342
			G99···O3	3.117	I100···C9	3.929
			T143···O11	2.791	H105···C1	4.477
			V146···O12	2.671	V118···C4	4.011
			G147···O12	2.93	A122···C2	3.253
			L148···O8	3.217	G129···C2	3.654
			K149···O6	2.701	T130···C3	3.729
			K368···O13	2.819		
			Mg^{2+}···O9	2.084		
			Mg^{2+}···O13	1.848		
Genistein	−4.62	−59.07	N144···O3	3.022	V63···C1	3.696
			N144···O2	2.969	G142···C9	3.68
			V146···O2	2.948	T143···C15	3.602
			G147···O2	3.207	G145···C3	3.84
			L148···O1	3.088	I304···C12	3.963
					V307···C11	4.354
					I361···C12	3.295
					W363···C14	3.435
					K368···C11	2.125

Fig. 5. Antiviral activity of genistein against ASFV Armenia/07 strain. (A) ASFV yield in macrophages treated with genistein in several concentrations. (B) Antiviral effect of genistein depending on the time of addition. (C) The DNA content of ASFV factories in genistein-treated macrophages. Values represent mean and standard deviation results from three independent experiments. Significant differences compared to control are denoted by *($P < 0.05$), **($P < 0.02$) and ***($P < 0.001$).

blocking viral immediate-early protein function (Evers et al., 2005) and Pichinde virus by disrupting the activation of the viral transcription factor-2 in Vero cells (Vela et al., 2008). Additionally, genistein was shown to suppress the replication of avian leukosis virus subgroup J by inhibiting virus transcription (Qian et al., 2014). Genistein can also inhibit HIV infection by blocking the viral protein U, which is believed to form ionic channels in the infected cell (Sauter et al., 2014).

We previously reported that ASFV was sensitive to genistein, though at concentrations that were toxic in this study (Hakobyan et al., 2016). Differences in non-toxic concentrations can be explained by the previously used method to measure cytotoxicity, crystal violet assay, which is less sensitive than MTT used in this study. Here we demonstrated that genistein at 50 μM concentration exhibited significant antiviral
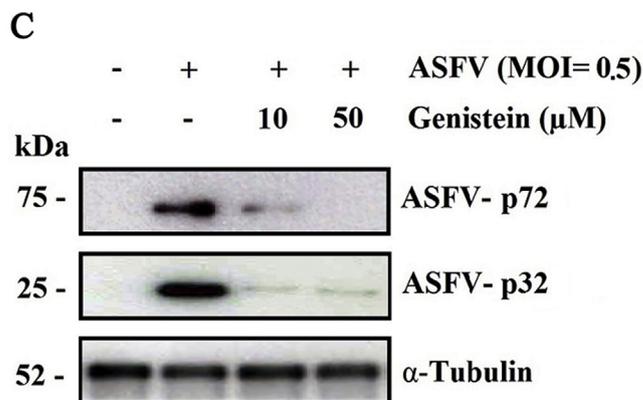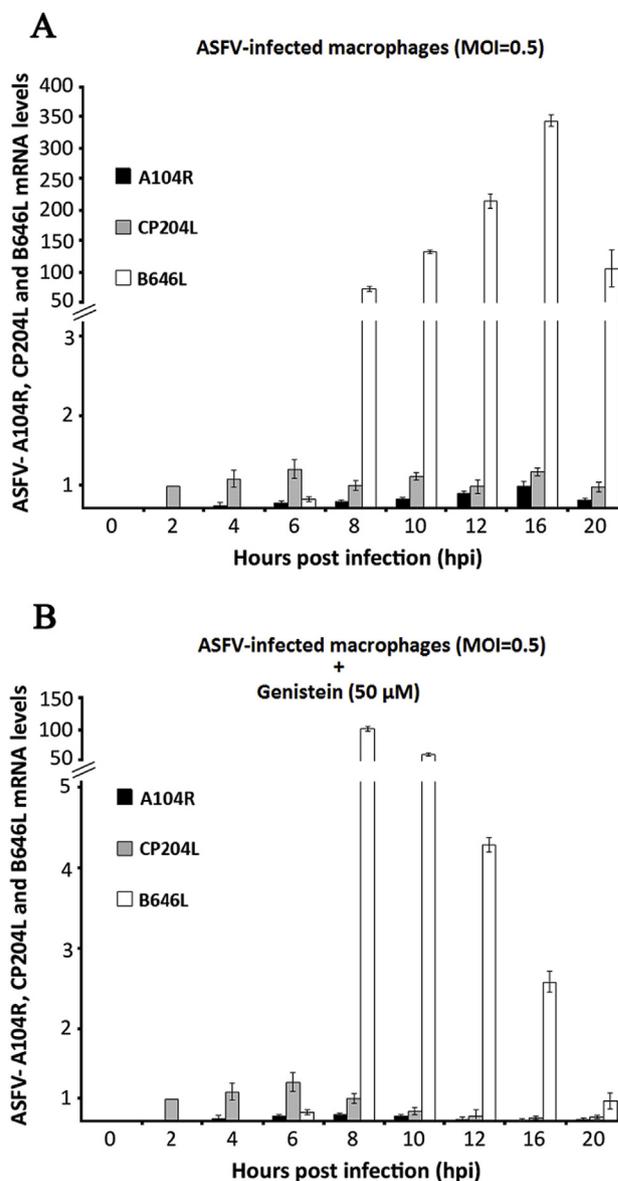
properties against ASFV infection *in vitro*, both in Vero cells and porcine macrophages. Antiviral assays revealed no virucidal effect on extracellular ASFV particles, as well as no interference in viral attachment and internalization steps. Furthermore, the pre-treatment of Vero cells with genistein also failed to inhibit ASFV infection, suggesting that this compound did not affect the host effectors or other regulatory factors.

Fig. 6. Genistein inhibits viral transcription and protein synthesis in macrophages infected with the ASFV-Armenia/07 strain. (A) qRT-PCR analysis of an early viral gene (CP204L) and two late genes (A104R, B646L), at different time points, after infection of porcine macrophages with the ASFV Armenia/07 isolate (MOI = 0.5). (B) Viral gene expression analysis of the same viral transcripts in ASFV-infected porcine macrophages treated with Genistein (50 μM) at 8 hpi, during 1 h. Mock-infected macrophages were used as a control in both assays. The results are shown as averages ± standard errors (SE) between the number of molecules of each viral gene and the number of molecules of the housekeeping gene Cyclophilin A. The results were obtained from three independent experiments. (C) Viral protein synthesis was analyzed in non-treated and genistein-treated porcine macrophages (10 μM and 50 μM), at 16 hpi. Molecular weights (kDa) of the evaluated viral proteins are indicated on the left of immunoblot image and the α-tubulin was used as a loading control.

These results indicated that genistein targeted the post-entry stages of ASFV infection, also supported by the fact that genistein showed higher efficiency when added at 8 hpi. This time point coincides with the initiation of the cytoplasmic phase of viral DNA replication (García-Beato et al., 1992; Rojo et al., 1999; Simões et al., 2015), and, therefore, we assumed that genistein could interfere with this process. For this reason, we quantified the DNA content in viral factories using image cytometry. The reduction of ASFV DNA in genistein-treated cells suggested that this compound inhibited viral DNA replication. This scenario was further supported by a reduction of viral gene expression and absence of the late viral protein p72 in porcine macrophages and Vero cells exposed to genistein, since it is known that expression of late viral genes does not occur in presence of viral DNA replication inhibitors (Rodríguez and Salas, 2013). The rapid metabolic inactivation and short half-life of genistein may explain why its inhibitory effect on DNA replication and viral yield was less profound, when it was added at early times post-infection (Chang et al., 2000; Yang et al., 2012).

Currently, there are several flavonoids that inhibit DNA and RNA virus by targeting enzymes involved in genome replication and transcription. For example, quercetin and myricetin are strong inhibitors of HIV reverse transcriptase (Ono et al., 1990), while wogonin has been shown to suppress duck hepatitis B virus (DHBV) DNA polymerase in infected ducks (Guo et al., 2007). Furthermore, myricetin and scutellarein inhibit SARS-coronavirus infection by affecting the ATPase activity of viral helicase protein (Yu et al., 2012). However, to our knowledge, there is no evidence that genistein may inhibit viral infection through interaction with enzymes involved in the process of viral DNA or RNA replication, although some early data suggested that genistein may stabilize the complex between topo II and DNA, thereby inducing topo II-mediated double-stranded breakage (Constantinou et al., 1990; Kiguchi et al., 1990). Recently, Coelho et al. (2016) showed that genistein at 32 μM concentration inhibited the activity of recombinant ASFV-topo II, purified from yeast. Based on these observations, we hypothesized that genistein interrupted ASFV DNA replication by inhibiting the viral topo II. Therefore, we expected a significant induction of DNA double-stranded breaks in ASFV-infected and genistein-treated cells. As expected, genistein was found to significantly induce DNA fragmentation, particularly at late phase (13 hpi) of infection. This phase is characterized by a high rate of ASFV DNA synthesis in Vero cells (Rojo et al., 1999). Thus, the inhibition of ASFV-topo II when it was more needed for viral genome replication caused a dramatic increase in topo II-mediated double-stranded breaks. Our hypothesis is further sustained by molecular docking analysis. Based on the fact that all members of topo II family are highly conserved proteins (Forterre and Gadelle, 2009; Forterre et al., 2007), we constructed ASFV-topo II homology model with two Mg^{2+} ions. We identified that genistein may interact with four amino acid residues in the predicted ATP-binding site with higher binding affinity than ATP^{4-}. All topo II enzymes catalyze changes in DNA topology in reactions coupled to the hydrolysis of ATP (Bates and Maxwell, 2010). Although it is unclear why topo II consumes ATP to support reactions that do not require

energy input, it has been proposed that the energy of ATP hydrolysis is needed to control the separation of protein-protein interfaces and prevent the accidental formation of double-stranded breaks (Bates et al., 2011). Therefore, the ATP-competitive inhibitors like genistein increase the rate of DNA fragmentation upon treatment. On the other hand, competition for the ATP-binding site should inhibit the rate of enzyme-catalyzed ATP hydrolysis. Indeed, early studies showed that genistein was a potent inhibitor of topo II-mediated ATP hydrolysis in *Drosophila melanogaster* Kc tissue culture cells (Robinson et al., 1993), suggesting that our docking results are in accordance with earlier findings.

Since the ATP-binding site of topo II is highly conserved among ASFV strains, genistein and other competitive inhibitors can be potent antivirals against virulent strains currently circulating in Africa and Eastern Europe. Here we showed that genistein was highly effective not only against avirulent ASFV Ba71V strain but also against ASFV Armenia/07 strain, which causes 100% mortality in domestic pigs. Thus, ASFV-topo II enzyme may be an excellent target for anti-ASFV agents. We suppose that greater effort should focus on the development of effective antiviral drugs that can be applied to treat infected pigs and thus to control the spread of infection. In developing a drug for pig health, there should be a necessary balance between the level of a compound's antiviral activity and the cost of preparing the compound. Therefore, the natural compounds like genistein are the center of our attention due to their high availabilities and low cost and side effects.

Appendix A. Supplementary data

Supplementary data related to this article can be found at http://dx.doi.org/10.1016/j.antiviral.2018.06.014.

References

Abagyan, R., Totrov, M., Kuznetsov, D., 1994. ICM—a new method for protein modeling and design: applications to docking and structure prediction from the distorted native conformation. J. Comput. Chem. 15, 488–506.

Argenta, D.F., Silva, I.T., Bassani, V.L., Koester, L.S., Teixeira, H.F., Simões, C.M., 2015. Antiherpes evaluation of soybean isoflavonoids. Arch. Virol. 160, 2335–2342.

Arias, M., de la Torre, A., Dixon, L., Gallardo, C., Jori, F., Laddomada, A., Martins, C., Parkhouse, R.M., Revilla, Y., Rodriguez, F., Sanchez-Vizcaino, J., 2017. Approaches and perspectives for development of African swine fever virus vaccines. Vaccines (Basel) 5 (4).

Bates, A.D., Berger, J.M., Maxwell, A., 2011. The ancestral role of ATP hydrolysis in type II topoisomerases: prevention of DNA double-strand breaks. Nucleic Acids Res. 39, 6327–6339.

Bates, A.D., Maxwell, A., 2010. The role of ATP in the reactions of type II DNA topoisomerases. Biochem. Soc. Trans. 38, 438–442.

Brooks, B.R., Bruccoleri, R.E., Olafson, B.D., States, D.J., Swaminathan, S.A., Karplus, M., 1983. CHARMM: a program for macromolecular energy, minimization, and dynamics calculations. J. Comput. Chem. 4, 187–217.

Carrascosa, A.L., Bustos, M.J., de Leon, P., 2011. Methods for growing and titrating African swine fever virus: field and laboratory samples. Curr. Protoc. Cell Biol. 26 26.14.

Chang, H.C., Churchwell, M.I., Delclos, K.B., Newbold, R.R., Doerge, D.R., 2000. Mass spectrometric determination of Genistein tissue distribution in diet-exposed Sprague-Dawley rats. J. Nutr. 130, 1963–1970.

Chiang, L.C., Ng, L.T., Cheng, P.W., Chiang, W., Lin, C.C., 2005. Antiviral activities of extracts and selected pure constituents of Ocimum basilicum. Clin. Exp. Pharmacol. Physiol. 32, 811–816.

Cho, W.K., Weeratunga, P., Lee, B.H., Park, J.S., Kim, C.J., Ma, J.Y., Lee, J.S., 2015. Epimedium koreanum Nakai displays broad spectrum of antiviral activity in vitro and in vivo by inducing cellular antiviral state. Viruses 7, 352–377.

Coelho, J., Ferreira, F., Martins, C., Leitão, A., 2016. Functional characterization and inhibition of the type II DNA topoisomerase coded by African swine fever virus.

Virology 493, 209–216.

Coelho, J., Martins, C., Ferreira, F., Leitão, A., 2015. African swine fever virus ORF P1192R codes for a functional type II DNA topoisomerase. Virology 474, 82–93.

Constantinou, A., Kiguchi, K., Huberman, E., 1990. Induction of differentiation and DNA strand breakage in human HL-60 and K-562 leukemia cells by genistein. Cancer Res. 50, 2618–2624.

Evers, D.L., Chao, C.F., Wang, X., Zhang, Z., Huong, S.M., Huang, E.S., 2005. Human cytomegalovirus-inhibitory flavonoids: studies on antiviral activity and mechanism of action. Antivir. Res. 68, 124–134.

Fernandez-Recio, J., Totrov, M., Skorodumov, C., Abagyan, R., 2005. Optimal docking area: a new method for predicting protein–protein interaction sites. Proteins 58, 134–143.

Forterre, P., Gadelle, D., 2009. Phylogenomics of DNA topoisomerases: their origin and putative roles in the emergence of modern organisms. Nucleic Acids Res. 37, 679–692.

Forterre, P., Gribaldo, S., Gadelle, D., Serre, M.C., 2007. Origin and evolution of DNA topoisomerases. Biochimie 89, 427–446.

Freitas, F., Frouco, G., Martins, C., Leitão, A., Ferreira, F., 2016. In vitro inhibition of African swine fever virus-topoisomerase II disrupts viral replication. Antivir. Res. 134, 34–41.

Frouco, G., Freitas, F.B., Coelho, J., Leitão, A., Martins, C., Ferreira, F., 2017. DNA-binding properties of African swine fever virus pA104R, a histone-like protein involved in viral replication and transcription. J. Virol. 91 e02498-16.

Gallardo, M.C., Reoyo, A.T., Fernández-Pinero, J., Iglesias, I., Muñoz, M.J., Arias, M.L., 2015. African swine fever: a global view of the current challenge. Porcine Health Manag. 1, 21.

García-Beato, R., Salas, M.L., Viñuela, E., Salas, J., 1992. Role of the host cell nucleus in the replication of African swine fever virus DNA. Virology 188, 637–649.

Guo, J., Xu, X., Rasheed, T.K., Yoder, A., Yu, D., Liang, H., Yi, F., Hawley, T., Jin, T., Ling, B., Wu, Y., 2013. Genistein interferes with SDF-1- and HIV-mediated actin dynamics and inhibits HIV infection of resting CD4 T cells. Retrovirology 10, 62.

Guo, Q., Zhao, L., You, Q., Yang, Y., Gu, H., Song, G., Lu, N., Xin, J., 2007. Anti-hepatitis B virus activity of wogonin in vitro and in vivo. Antivir. Res. 74, 16–24.

Hakobyan, A., Arabyan, E., Avetisyan, A., Abroyan, L., Hakobyan, L., Zakaryan, H., 2016. Apigenin inhibits African swine fever virus infection in vitro. Arch. Virol. 161, 3445–3453.

Hakobyan, A., Galindo, I., Nañez, A., Arabyan, E., Karalyan, Z., Chistov, A.A., Streshnev, P.P., Korshun, V.A., Alonso, C., Zakaryan, H., 2018. Rigid amphipathic fusion inhibitors demonstrate antiviral activity against African swine fever virus. J. Gen. Virol. 99, 148–156.

Huang, H., Liao, D., Liang, L., Song, L., Zhao, W., 2015. Genistein inhibits rotavirus replication and upregulates AQP4 expression in rotavirus-infected Caco-2 cells. Arch. Virol. 160, 1421–1433.

Johari, J., Kianmehr, A., Mustafa, M.R., Abubakar, S., Zandi, K., 2012. Antiviral activity of baicalein and quercetin against the Japanese encephalitis virus. Int. J. Mol. Sci. 13, 16785–16795.

Kiguchi, K., Constantinou, A.I., Huberman, E., 1990. Genistein-induced cell differentiation and protein-linked DNA strand breakage in human melanoma cells. Cancer Commun. 2, 271–277.

Laskowski, R.A., MacArthur, M.W., Moss, D.S., Thornton, J.M., 1993. PROCHECK: a program to check the stereochemical quality of protein structures. J. Appl. Crystallogr. 26, 283–291.

Lyu, S.Y., Rhim, J.Y., Park, W.B., 2005. Antiherpetic activities of flavonoids against herpes simplex virus type 1 (HSV-1) and type 2 (HSV-2) in vitro. Arch Pharm. Res. 28, 1293–1301.

Ono, K., Nakane, H., Fukushima, M., Chermann, J.C., Barré-Sinoussi, F., 1990. Differential inhibitory effects of various flavonoids on the activities of reverse transcriptase and cellular DNA and RNA polymerases. Eur. J. Biochem. 190, 469–476.

Qian, K., Gao, A.J., Zhu, M.Y., Shao, H.X., Jin, W.J., Ye, J.Q., Qin, A.J., 2014. Genistein inhibits the replication of avian leucosis virus subgroup J in DF-1 cells. Virus Res. 192, 114–120.

Robinson, M.J., Corbett, A.H., Osheroff, N., 1993. Effects of topoisomerase II-targeted drugs on enzyme-mediated DNA cleavage and ATP hydrolysis: evidence for distinct drug interaction domains on topoisomerase II. Biochemistry 32, 3638–3643.

Rodríguez, J.M., Salas, M.L., 2013. African swine fever virus transcription. Virus Res. 173, 15–28.

Rojas, Á., Del Campo, J.A., Clement, S., Lemasson, M., García-Valdecasas, M., Gil-Gómez, A., Ranchal, I., Bartosch, B., Bautista, J.D., Rosenberg, A.R., Negro, F., Romero-Gómez, M., 2016. Effect of quercetin on hepatitis C virus life cycle: from viral to host targets. Sci. Rep. 6, 31777.

Rojo, G., García-Beato, R., Viñuela, E., Salas, M.L., Salas, J., 1999. Replication of African swine fever virus DNA in infected cells. Virology 257, 524–536.

Romano, B., Pagano, E., Montanaro, V., Fortunato, A.L., Milic, N., Borrelli, F., 2013. Novel insights into the pharmacology of flavonoids. Phytother Res. 27, 1588–1596.

Sauter, D., Schwarz, S., Wang, K., Zhang, R., Sun, B., Schwarz, W., 2014. Genistein as antiviral drug against HIV ion channel. Planta Med. 80, 682–687.

Schapira, M., Totrov, M., Abagyan, R., 1999. Prediction of the binding energy for small molecules, peptides and proteins. J. Mol. Recogn. 12, 177–190.

Simões, M., Martins, C., Ferreira, F., 2015. Early intranuclear replication of African swine fever virus genome modifies the landscape of the host cell nucleus. Virus Res. 210, 1–7.

Tice, R.R., Agurell, E., Anderson, D., Burlinson, B., Hartmann, A., Kobayashi, H., Miyamae, Y., Rojas, E., Ryu, J.C., Sasaki, Y.F., 2000. Single cell gel/comet assay: guidelines for in vitro and in vivo genetic toxicology testing. Environ. Mol. Mutagen. 35, 206–221.

Totrov, M., Abagyan, R., 1997. Flexible protein–ligand docking by global energy optimization in internal coordinates. Proteins 29 (S1), 215–220.

Vela, E.M., Bowick, G.C., Herzog, N.K., Aronson, J.F., 2008. Genistein treatment of cells inhibits arenavirus infection. Antivir. Res. 77, 153–156.

Yang, Z., Kulkarni, K., Zhu, W., Hu, M., 2012. Bioavailability and pharmacokinetics of genistein: mechanistic studies on its ADME. Anticancer Agents Med. Chem. 12, 1264–1280.

Yu, M.S., Lee, J., Lee, J.M., Kim, Y., Chin, Y.W., Jee, J.G., Keum, Y.S., Jeong, Y.J., 2012. Identification of myricetin and scutellarein as novel chemical inhibitors of the SARS coronavirus helicase, nsP13. Bioorg. Med. Chem. Lett 22, 4049–4054.

Zakaryan, H., Revilla, Y., 2016. African swine fever virus: current state and future perspectives in vaccine and antiviral research. Vet. Microbiol. 185, 15–19.